Comparative Study of Diastereoisomer Interconversion in Chiral BINOL-ate and Diamine Platinum Complexes of Conformationally Flexible NUPHOS Diphosphines

Simon Doherty,*,† Colin R. Newman,† Rakesh K. Rath,†
Jan-Albert van den Berg,† Christopher Hardacre,† Mark Nieuwenhuyzen,† and
Julian G. Knight*,‡

Centre for the Theory and Applications of Catalysis, School of Chemistry, The Queen's University of Belfast, David Keir Building, Stranmillis Road, Belfast BT9 5AG, U.K., and School of Natural Sciences, Chemistry, Bedson Building, The University of Newcastle upon Tyne, Newcastle upon Tyne NE1 7RU, U.K.

Received November 11, 2003

A thorough and detailed study of diastereointerconversion in the chiral platinum complexes [(NUPHOS)Pt{(*S*)-BINOL}] (**3a**−**e**) has been undertaken and compared with the results of a similar study with [(BIPHEP)Pt{(*S*)-BINOL}]. Rate data revealed that this process obeys first-order relaxation kinetics, and rate constants for conversion of the minor to the major diastereoisomer have been obtained. Eyring analysis of the data gave $\Delta H^{\ddagger}$ and $\Delta S^{\ddagger}$ values of 22−25 kcal mol^{-1} and −1 to −16 eu, respectively. In combination with computational analysis, these studies indicate that atropinversion most likely occurs via an on-metal pathway involving a planar seven-membered transition state. Substitution of (*S*)-BINOL for (*S*,*S*)-DPEN results in a marked reduction in the barrier to atropinversion; a $\Delta H^{\ddagger}$ value of 17 kcal mol^{-1} has been determined for the conversion of δ-[(Ph_4-NUPHOS)Pt{(*S*,*S*)-DPEN}]-Cl_2 to λ-[(Ph_4-NUPHOS)Pt{(*S*,*S*)-DPEN}]Cl_2, which could indicate that an alternative mechanism operates.

Introduction

Traditionally, the design of new chiral catalysts has been guided by the concept that a conformationally restricted enantiopure ligand is necessary to achieve high enantioselectivities in asymmetric transformations.[1] Recently, though, Mikami and Noyori have demonstrated that the conformationally flexible *tropos* diphosphine 2,2′-bis((3,5-dimethylphenyl)phosphino)biphenyl (DM-BIPHEP) can be used for the enantioselective ruthenium-catalyzed reduction of 1-acetonaphthone, a strategy now termed asymmetric activation.[2] In this experiment addition of (*S*,*S*)-1,2-diphenylethylenediamine (*S*,*S*-DPEN) to [$RuCl_2$(DM-BIPHEP)$(dmf)_n$] gave [$RuCl_2$(DM-BIPHEP){(*S*,*S*)-DPEN}] as a 1:1 mixture of diastereoisomers, which underwent atropisomerism to a 3:1 thermodynamic mixture at 80 °C in 2-propanol/chloroform. The relative population of the two BIPHEP conformations has a dramatic influence on catalyst performance, the 1:1 and 3:1 *S*/*S*,*S*:*R*/*S*,*S* mixtures giving (*R*)-1-(1-naphthyl)ethanol in 63% and 84% ee, respectively. A further increase in enantioselectivity was obtained at low temperature, the 3:1 diastereoenriched mixture giving 92% ee; this is a significant improvement on the performance of the corresponding racemic BINAP derivative. The population of BIPHEP conformations and hence catalyst performance can be influenced by introducing substituents at the 3,5-positions of BIPHEP and/or the nitrogen atoms of DPEN.[3] For example, the *R*/*S*,*S* diastereoisomer of a 1:1 mixture of [$RuCl_2$(BIPHEP){(*S*,*S*)-dimethyl-DPEN}] epimerizes completely to give diastereoisomerically pure [$RuCl_2$(*S*-BIPHEP){(*S*,*S*)-dimethyl-DPEN}] at 50 °C in propan-2-ol.

In an attempt to investigate the mechanism of atropinversion, Gagné has studied diastereoisomer interconversion in the chiral complexes [(BIPHEP)Pt{(1*R*,2*S*)-OCHPhCHPhNTf}] and [(BIPHEP)Pt{(*S*)-BINOL}] (eq 1) and shown that coordination of BIPHEP to a substitutionally inert metal center, such as platinum(II), significantly slows atropinversion compared with the

* Corresponding author.
† The Queen's University of Belfast.
‡ The University of Newcastle upon Tyne.

(1) (a) Seyden-Penne, J. *Chiral Auxiliaries and Ligands in Asymmetric Catalysis*; Wiley: New York, 1995. (b) Noyori, R. *Asymmetric Catalysis in Organic Synthesis*; Wiley: New York, 1994. (c) Ojima, I., Ed. *Catalytic Asymmetric Synthesis,* 2nd ed.; Wiley-VCH: New York, 2000.

(2) (a) Mikami, K.; Korenaga, T.; Terada, M.; Ohkuma, T.; Pham, T.; Noyori, R. *Angew. Chem., Int. Ed.* **1999**, *38*, 495. For recent informative reviews see: (b) Walsh, P. J.; Lurain, A. E.; Balsells, J. *Chem. Rev.* **2003**, *103*, 3297. (c) Mikami, K.; Aikawa, K.; Yusa, Y.; Jodry, J. J.; Yamanaka, M. *Synlett* **2002**, 1561. (d) Mikami, K.; Terada, M.; Korenaga, T.; Matsumoto, Y.; Matsukawa, S. *Acc. Chem. Res.* **2000**, *33*, 391. (e) Mikami, K.; Terada, M.; Korenaga, T.; Matsumoto, Y.; Ueki, M.; Angeland, R. *Angew. Chem., Int. Ed.* **2000**, *39*, 3532.

(3) Korenaga, T.; Aikawa, K.; Terada, M.; Kawauchi, S.; Mikami, K. *Adv. Synth. Catal.* **2001**, *343*, 284.

10.1021/om034289f CCC: $27.50
Publication on Web 01/30/2004

octahedral [(BIPHEP)$RuCl_2${(*S*,*S*)-DPEN}] catalyst.[4]

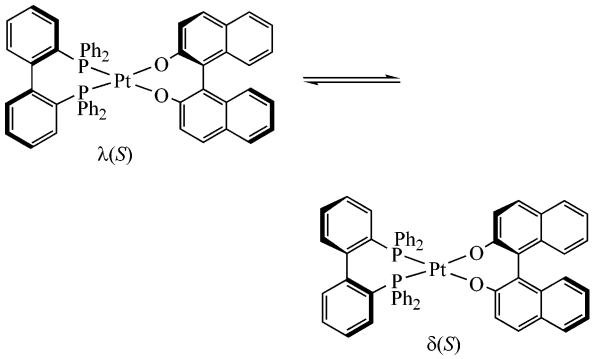

(1)

This increase in barrier to atropisomerism was used to resolve enantiopure *λ*-(BIPHEP)$PtCl_2$ and *δ*-(BIPHEP)-$PtCl_2$, by treatment of the corresponding *λ*(*S*) and 95:5 *δ*(*S*) diastereopure [(BIPHEP)Pt{(*S*)-BINOL}] with HCl.[5] Treatment of diastereopure [(BIPHEP)Pt{(*S*)-BINOL}] with trifluoromethanesulfonic acid or homochiral [(BIPHEP)$PtCl_2$] with silver triflate was used to generate the corresponding enantiopure Lewis acid complexes *λ*-(BIPHEP)Pt^{2+} and *δ*-(BIPHEP)Pt^{2+}, which catalyze the Diels−Alder and glyoxylate-ene reactions. The high ee's obtained in both reactions clearly demonstrate that conformationally flexible diphosphines can be used as effective chiral auxiliaries to achieve high enantioselectivities in asymmetric catalysis. Mikami adopted a similar strategy to isolate enantio- and diastereomerically pure palladium complexes of BIPHEP, relying on coordination of (*R*)-diaminobinaphthyl ((*R*)-DABN)) to generate a diastereoisomeric mixture of [Pd{BIPHEP}-{(*R*)-DABN}][SbF_6]$_2$.[6] Atropinversion at 80 °C for 12 h gave the thermodynamically favored [Pd{(*R*)-BIPHEP}-{(*R*)-DABN}][SbF_6]$_2$, which acts as an activated catalyst for the hetero Diels−Alder reaction between 1,3-cyclohexadiene and ethyl glyoxylate to give ee values as high as 94%. A similar strategy has been successfully applied to control the axial chirality of bis(diphenylphosphino)-ferrocene to effect the nickel-catalyzed asymmetric glyoxylate-ene reaction.[7]

Asymmetric activation using a conformationally flexible diphosphine to achieve high enantioselectivities is an attractive strategy, since it offers immense scope for structural variation and catalyst tuning. In this regard, we have recently reported the synthesis of an entirely new class of conformationally flexible diphosphine, NUPHOS (Chart 1), based on two diphenylphosphino groups linked by a four-carbon sp^2-hybridized tether, which clearly fulfills the criteria of a conformationally flexible diphosphine capable of undergoing atropisomerism.[8] Asymmetric activation and on-metal resolution

Chart 1

1,2,3,4-R_4-NUPHOS

R = Me, **1a**; R = Et; **1b**
R = Ph; **1c**

1,4-R_2-2,3-*cyclo*-C_6H_8-NUPHOS

R = Et, **1d**; R = Ph; **1e**

using conformationally flexible NUPHOS-type diphosphines are promising alternative approaches to the use of their enantiopure counterparts, since a wide range of alkynes and diynes either are commercially available or can be prepared via relatively straightforward inexpensive procedures. Since we ultimately intend to investigate the use of NUPHOS-type diphosphines in platinum-group-catalyzed asymmetric transformations,[9] via either asymmetric activation or chiral environment amplification, we have examined their coordination chemistry and determined the rate of atropinversion with the aim of understanding the mechanism of this process. Herein we report the results of our studies in this area, including a kinetic study of diastereoisomer interconversion in the chiral platinum complexes [(NUPHOS)Pt{(*S*)-BINOL}] and [(Ph_4−NUPHOS)Pt-{(*S*,*S*)-DPEN}]Cl_2.

Results and Discussion

Synthesis and Characterization of [(NUPHOS)-$PtCl_2$] (2a−e) and [(NUPHOS)Pt{(*S*)-BINOL}] (3a−e). Slow addition of a dichloromethane solution of **1a**−**e** into a dichloromethane solution of [(cycloocta-1,5-diene)-$PtCl_2$] resulted in the rapid appearance of a yellow coloration with the formation of [(NUPHOS)$PtCl_2$] (**2a**−**e**) in yields of up to 88%. Compounds **2a**−**e** have been characterized using standard spectroscopic techniques and, in the case of **2a**, by a single-crystal X-ray study. For each compound, the ^{31}P NMR spectrum contains a single sharp signal flanked by platinum satellites, with J_{Pt-P} between 3607 and 3814 Hz, in the region expected for a phosphine trans to chloride.[10] The ^1H NMR spectra of compounds **2a**−**e** each contain at least one distinctive low-field-shifted exchange-broadened signal, as a result of restricted rotation of the diphenylphosphino phenyl rings,[8b] together with numerous well-resolved multiplets associated with the remaining aromatic protons. Compounds **3a**−**e** (Chart 2) were prepared as near 1:1 mixtures of enantiopure diastereoisomers by following a procedure similar to that recently reported by Gagné and co-workers.[10] Dropwise addition of a THF solution of Na_2-(*S*)-BINOL, generated in situ by deprotonation of (*S*)-BINOL with sodium *tert*-butoxide, to a suspension

(4) Tudor, M. D.; Becker, J. J.; White, P. S.; Gagné, M. R. *Organometallics* **2000**, *19*, 4376.

(5) (a) Becker, J. J.; White, P. S.; Gagné, M. R. *J. Am. Chem. Soc.* **2001**, *123*, 9478. (b) Brunkan, N. M.; Gagné, M. R. *Organometallics* **2002**, *21*, 1576. (c) Brunkan, N. M.; White, P. S.; Gagné, M. R. *Organometallics* **2002**, *21*, 1565.

(6) (a) Mikami, K.; Aikawa, K.; Yusa, Y.; Hatano, M. *Org. Lett.* **2002**, *4*, 91. (b) Mikami, K.; Aikawa, K.; Yusa, Y. *Org. Lett.* **2002**, *4*, 95.

(7) Mikami, K.; Aikawa, K. *Org. Lett.* **2002**, *4*, 99.

(8) (a) Doherty, S.; Knight. J. G.; Robins, E. G.; Scanlan, T. H.; Champkin, P. A.; Clegg, W. *J. Am. Chem. Soc.* **2001**, *123*, 5110. (b) Doherty, S.; Robins, E. G.; Nieuwenhuyzen, M.; Knight, J. G.; Champkin, P. A.; Clegg, W. *Organometallics* **2002**, *21*, 1383. (c) Doherty, S.; Newman, C. R.; Hardacre, C.; Nieuwenhuyzen, M.; Knight, J. G. *Organometallics* **2003**, *22*, 1452.

(9) (a) Doherty, S.; Newman, C. R.; Rath, R. K.; Luo, H.-K.; Nieuwenhuyzen, M.; Knight, J. G. *Org. Lett.* **2003**, 3863. (b) Ghosh, A. K.; Matsuda, H. *Org. Lett.* **1999**, *1*, 2157. (c) Hao, J.; Hatano, M.; Mikami, K. *Org. Lett.* **2000**, *2*, 4059. (d) Hori, K.; Kodana, H.; Ohta, T.; Furukawa, I. *J. Org. Chem.* **1999**, *64*, 5017. (e) Hori, K.; Ohta, T.; Furukawa, I. *Tetrahedron* **1998**, *64*, 12737. (f) Sodeoka, M.; Ryosuke, T.; Miyazaki, F.; Hagiwara, E.; Shibasaki, M. *Synlett* **199**7, 463. (g) Oi, S.; Terada, E.; Ohuchi, K.; Kato, T.; Tachibana, Y.; Inoue, Y. *J. Org. Chem.* **1999**, *64*, 8660. (h) Hamashima, Y.; Hotta, D.; Sodeoka, M. J. *Am. Chem. Soc.* **2002**, *124*, 11240.

(10) (a) Mather, G. G.; Pidcock, A.; Rapsey, G. J. N. *J. Chem. Soc., Dalton Trans.* **1973**, 2095. (b) Pidcock, A. *Adv. Chem. Ser.* **1982**, *196*, 1.

Chart 2

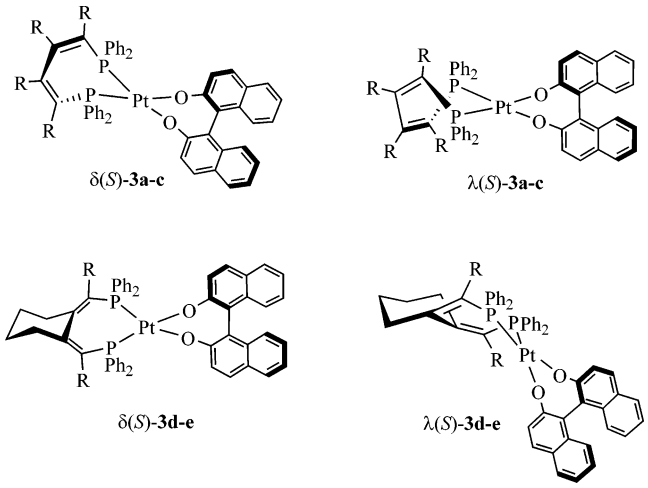

Scheme 1

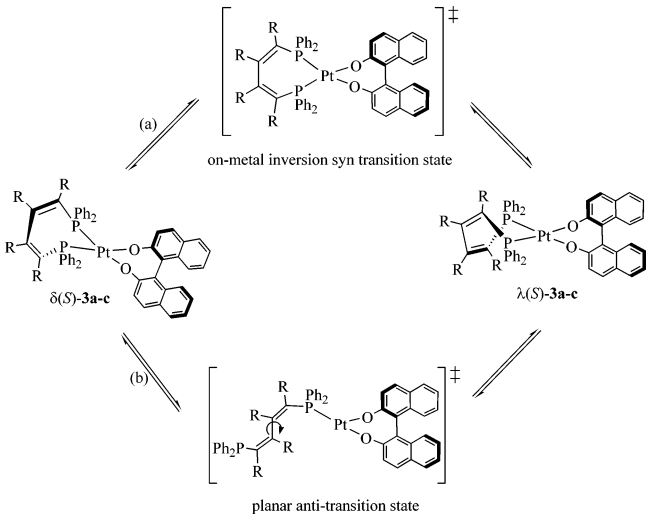

of **2a**−**e** in toluene resulted in the immediate appearance of an intense orange or yellow color, characteristic of the desired product. The reaction is typically complete within 2−3 h, and the product was routinely isolated in high yield. The ^{31}P NMR spectra of **3a**−**e** each contain two singlets which correspond to $\lambda(S)$-**3a**−**e** and $\delta(S)$-**3a**−**e** with platinum satellite coupling constants, J_{Pt-P}, between 3619 and 3700 Hz, very similar to the corresponding values in **2a**−**e**. While the thermodynamically preferred diastereoisomers of **3b**−**e**, $\delta(S)$, were obtained by thermolysis of a toluene solution overnight followed by recrystallization, the thermodynamically less favored diastereoisomer of **3a**, $\lambda(S)$, has been isolated pure by fractional crystallization from a 1:1 diastereoisomeric mixture at room temperature. A ^{31}P NMR spectrum of a representative sample of λ-**3a** confirmed that only the thermodynamically less stable diastereoisomer crystallized and that it undergoes atropinversion at elevated temperatures to give the thermodynamically more stable diastereoisomer.

A sample of the diastereopure δ-[(Ph_4-NUPHOS)Pt{(*S*,*S*)-DPEN}]Cl_2 (**4·Cl$_2$**), required for the kinetic study, was prepared by reaction of enantiopure δ-[(Ph_4-NUPHOS)$PtCl_2$][9a] with (*S*,*S*)-DPEN in dichloromethane (eq 2). Reaction was complete within 5 min, after which

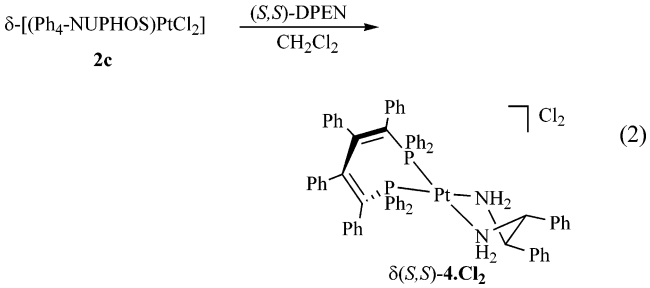

(2)

time the solution was filtered, the solvent removed, and the resulting residue triturated with hexane to give δ-(*S*,*S*)-**4·Cl$_2$** as a spectroscopically pure pale yellow powder. The ^{31}P NMR spectrum of **4·Cl$_2$** contains a triplet at δ −6.5 with $^1J_{Pt-P}$ = 3315 Hz, and the ^{1}H NMR spectrum contains two set of multiplets associated with the amino protons and another belonging to the methine protons of the diamine backbone. After the compound stood in chloroform for several hours, a second set of multiplets began to appear, which were shown to correspond to the thermodynamically more stable diastereoisomer λ-[(Ph_4-NUPHOS)Pt{(*S*,*S*)-DPEN}]Cl_2 (Table 1), unequivocally confirming that δ-NUPHOS and (*S*,*S*)-DPEN have mismatched stereochemistries.

Kinetic Study of Diastereoisomer Interconversion of [(NUPHOS)Pt{(*S*)-BINOL}] (3a−e). Since the use of conformationally flexible diphosphines such as BIPHEP and NUPHOS in asymmetric catalysis relies on the slow interconversion of chiral conformations, several experimental and theoretical studies have been undertaken in an attempt to distinguish between the two possible pathways: (i) on-metal inversion passing through the s-cis diene conformation of a seven-membered metallacycle (Scheme 1a) and (ii) M−P bond dissociation involving either an s-trans or s-cis conformation (Scheme 1b). On the basis of the relative rates of diastereointerconversion in ruthenium and platinum complexes of BIPEHP, Gagné recently presented compelling arguments for dissociation-induced biaryl rotation but conceded that on-metal atropinterconversion could not be dismissed.[11] Unfortunately, the kinetic data obtained in a detailed and thorough study of diastereointerconversion in the chiral complexes [(BIPHEP)PtX_2] (X_2 = N(Tf)CHPhCHPhO, (*S*)-BINOL) could not distinguish between these two possible mechanisms.[4] Pyridine was shown to lower the isomerization temperature of enantiopure λ-[(BIPHEP)Pt{(*S*)-BINOL}] by ca. 50 °C, which was tentatively suggested to be due to an enhanced rate of phosphine dissociation in a five-coordinate pyridine intermediate. In the case of atropointerconversion of (*S*/*S*,*S*)- and (*R*/*S*,*S*)-[Ru(BIPHEP)Cl_2-{(*S*,*S*)-DPEN}], theoretical studies support a mechanism involving solvent-assisted dissociation of one of the Ru−P bonds, rotation about the biphenyl single bond, and subsequent recoordination of phosphine.[12] We have investigated the process of atropinterconversion in **3a**−**e**, reasoning that the geometrical difference between the four-carbon tethers in **3a**−**c** and **3d**,**e** might manifest itself in the activation parameters for atropintercon-

(11) (a) Alguindigue, A. S.; Khan, M. A.; Ashby, M. T. *Organometallics* **1999**, *18*, 5112. (b) Ashby, M. T.; Alguindigue, A. S.; Khan, M. A. *Organometallics* **2000**, *19*, 547. (c) Ashby, M. T. *J. Am. Chem. Soc.* **1995**, *117*, 2000. (d) Ashby, M. T.; Govindan, G. N.; Groftan, A. K. *J. Am. Chem. Soc.* **1994**, *116*, 4801.

(12) Yamanaka, M.; Mikami, K. *Organometallics* **2002**, *21*, 5847.

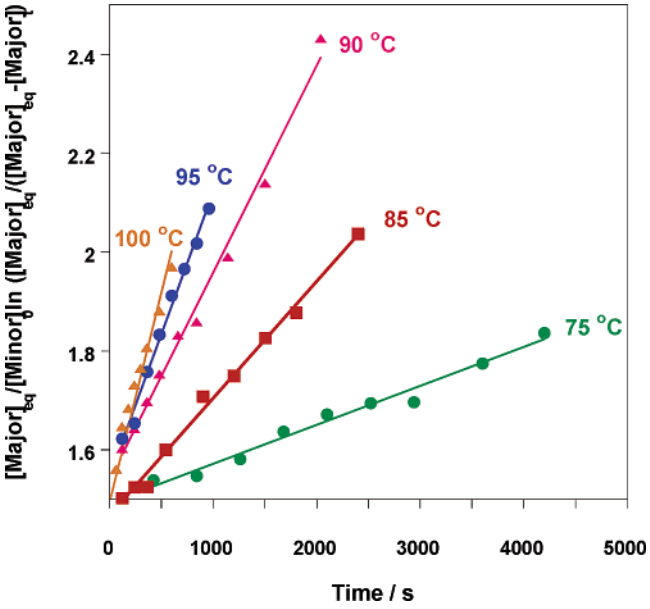

Figure 1. Reversible first-order analyses for the thermal conversion of $\lambda(S)$-**3a** to $\delta(S)$-**3a** in toluene−chlorobenzene (7:3). First-order analyses for the conversions of $\lambda(S)$-**3b**−**d** to $\delta(S)$-**3b**−**d** and of δ(S,*S*)-**4·Cl₂** to λ(S,*S*)-**4·Cl₂** are given in the Supporting Information.

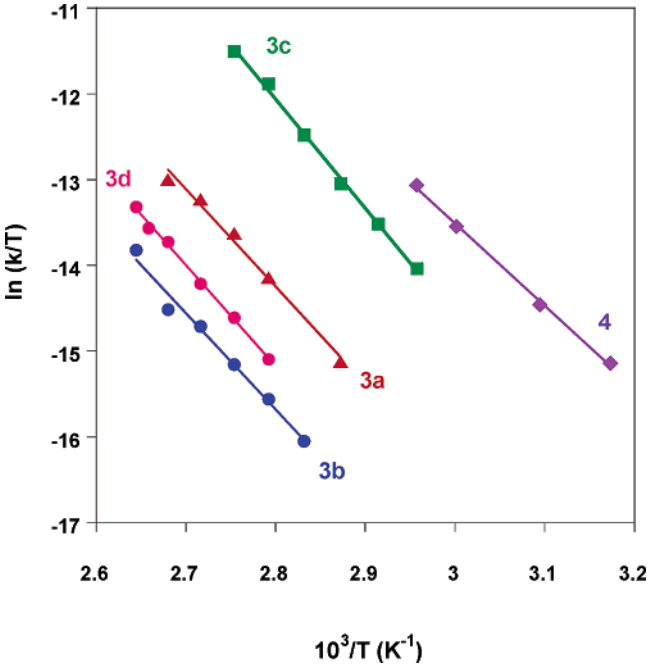

Figure 2. Eyring analysis of the rate data obtained for the thermal conversion of $\lambda(S)$-**3a**−**d** to $\delta(S)$-**3a**−**d** and of δ(S,*S*)-**4·Cl₂** to λ(S,*S*)-**4·Cl₂**.

version, since the latter necessarily involves inversion of a cyclohexane ring, which is expected to have a higher barrier to activation than rotation about the C(2)−C(3) bond of an acyclic 1,3-butadiene and which cannot undergo anti rotation in the same manner as BIPHEP and related diphosphines. Thus, a comparative study of diastereointerconversion of **3a**−**e** might indicate which of the two pathways commonly associated with atropisomerism operates.

Table 1. Activation Parameters for the Atropisomerization of Compounds 3a−d and 4

param (error)	3a	3b	3c	3d	4·Cl₂
$\Delta H^{\ddagger}$, kcal mol^{-1} (3)	23	22	25	23	17
$\Delta S^{\ddagger}$, eu (8)	−12	−16	−1	−12	−23
δ/λ equilibrium ratio at 85 °C	3.8	19.1	11.1	11.1	0.34[a]

[a] Equilibrium constant at 65 °C.

Thermolysis of a chlorobenzene/toluene solution of a 1:1 mixture of enantiopure $\lambda(S)$-**3a**−**e** and $\delta(S)$-**3a**−**e** within a narrow temperature range resulted in clean conversion to a thermodynamic equilibrium ratio containing a major and a minor diastereoisomer (Table 1). The interconversion was conveniently monitored by ^{31}P NMR spectroscopy, which was used to acquire kinetic data for the atropinversion. Analysis of the data revealed that the process obeys reversible first-order relaxation kinetics. Figure 1 shows the reversible first-order analysis for the interconversion of a 1:1 mixture of $\lambda(S)$-**3a** and $\delta(S)$-**3a** using the integrated rate expression for a standard reversible first-order process (A ↔ B).[13,14] Eyring analyses of the rate data obtained for atropinversion of **3a**−**d** gave $\Delta H^{\ddagger}$ in the range 22−25 kcal mol^{-1} and $\Delta S^{\ddagger}$ between −1 and 16 eu, full details of which are listed in Table 1 and presented in Figure 2. During similar experiments with **3e**, significant decomposition occurred after prolonged heating, and equilibrium values were not obtainable. An estimate of $\Delta H^{\ddagger}$ for **3e** using the equilibrium values for **3d** gave 23 kcal mol^{-1}: i.e., within the range for **3a**−**d.** The data in Table 1 clearly reveal that the activation parameters for atropinversion of **3a**−**c** are similar to that for **3d**,**e**, which strongly suggests that complexes of acyclic and monocyclic NUPHOS diphosphines undergo atropinversion via the same pathways. Since the cyclohexyl ring in monocyclic NUPHOS diphosphines prevents anti rotation, the only two possible pathways for atropinversion are on-metal involving a syn transition state or dissociation-induced rotation also via a syn transition state. Moreover, these activation parameters are similar to those recently reported by Gagné for the thermal conversion of $\lambda(S)$-[(BIPHEP)Pt(BINOL)] to $\delta(S)$-[(BIPHEP)Pt(BINOL)] ($\Delta H^{\ddagger} = 27(2)$ kcal mol^{-1}, $\Delta S^{\ddagger} = -5(5)$ eu). In the case of compound **3a**, a van't Hoff analysis of the equilibrium data obtained from the thermolysis experiment gave $\Delta H° = 0.8$ kcal mol^{-1} and $\Delta S° = 5$ eu (Figure 3), which is a clear measure of the relative thermodynamic stability of the matched and mismatched diastereoisomers. In the case of **3a** an equilibrium ratio of 75:25 was observed for $\delta(S)$-**3a**:$\lambda(S)$-**3a**, whereas the corresponding ratios for compounds **3b**−**e** are all much closer to 95:5. Solutions of diastereopure $\delta(S)$-**3c** do not show any sign of diastereointerconversion at room temperature even after standing for 24 h, which is consistent with the experimentally determined barrier of 25 kcal mol^{-1} for atropinversion of $\lambda(S)$-**3c** to $\delta(S)$-**3c**.

In considering the on-metal mechanism, Gagné has argued that the greater rate of atropinterconversion for [(BIPHEP)RuCl$_2${(*S*,*S*)-DPEN}] compared with [(BIPHEP)Pt{(*S*)-BINOL}] could be caused by steric interactions between the apical chlorides and the pseudoaxial

(13) $([B]_{eq}/[A]_0)[\ln([B]_{eq}/[B]_{eq} - [B]_t)] = kt$: Laidler, K. J. *Chemical Kinetics*, 3rd ed.; Harper & Row: New York, 1987.

(14) First-order rate constants obtained for the diastereointerconversion of compounds **3a**−**d** and **4·Cl₂** are listed in Table S1 of the Supporting Information.

Scheme 2

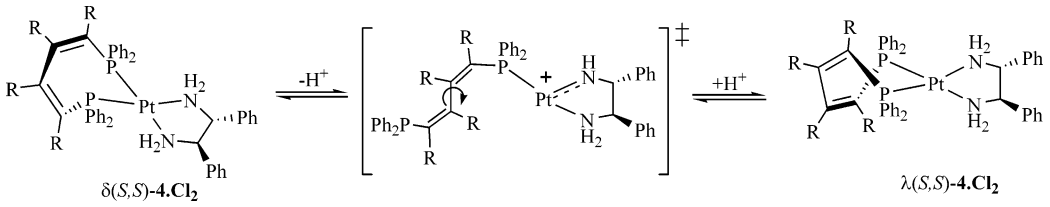

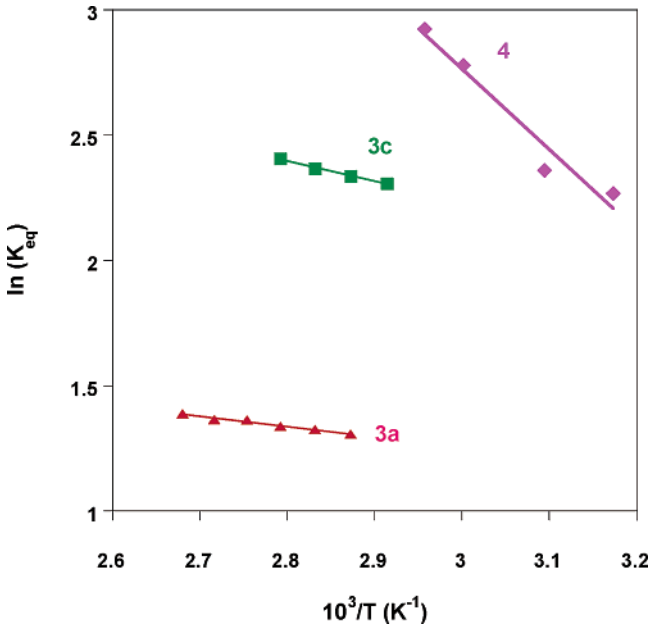

Figure 3. van't Hoff analyses of the equilibrium data obtained from the thermal conversion of $\lambda(S)$-**3a** to $\delta(S)$-**3a**, of $\lambda(S)$-**3c** to $\delta(S)$-**3c**, and of $\delta(S,S)$-**4·Cl₂** to $\lambda(S,S)$-**4·Cl₂**.

phenyl groups, which would raise the ground-state energy. To investigate this possibility, we have studied diastereointerconversion in the corresponding diphosphine−diamine complex [(Ph_4-NUPHOS)Pt{(*S*,*S*)-DPEN}]Cl_2 (**4·Cl₂**). Eyring analysis of the rate data obtained for interconversion of δ-[(Ph_4-NUPHOS)Pt{(*S*,*S*)-DPEN)}]Cl_2 to λ-[(Ph_4-NUPHOS)Pt{(*S*,*S*)-DPEN}]Cl_2 revealed that atropinterconversion is significantly more rapid in **4·Cl₂** compared to **3a**−**e**, with activation parameters of $\Delta H^{\ddagger} = 17$ kcal mol^{-1} and $\Delta S^{\ddagger} = -23$ eu (Figure 2). A van't Hoff analysis of the equilibrium data obtained from the thermolysis of $\delta(S,S)$-**4·Cl₂** (Figure 3) gave a $\Delta H°$ value of 2.5 kcal mol^{-1} compared with 1.6 kcal mol^{-1} for its BINOL-ate counterpart **3c**. It is clear from the temperature dependence of K_{eq} for **3c** and **4·Cl₂** (Figure 3) that both the choice of chiral activator (DPEN versus BINOL) and the temperature are important for optimizing resolution using diastereoisomeric complexes, since a large K_{eq} value is most desirable in the absence of kinetic resolution. The larger $\Delta H°$ for **4·Cl₂** compared with **3c**, for example, means that in order to obtain the optimum diastereoisomeric ratio and ultimately yield, the resolution of Ph_4-NUPHOS with (*S*,*S*)-DPEN would be most effective at elevated temperatures, whereas there would be no significant advantage in performing the BINOL-ate-based resolution at high temperature; lower temperatures would also decrease the possibility of decomposition. Similar considerations are also likely to apply to the use of diastereoisomeric complexes in asymmetric catalysis, and the use of conformationally flexible 2,2′-bis(diarylphosphino)-1,1′-biphenyl phosphines in combination with chiral diamines for the ruthenium-catalyzed enantioselective hydrogenation is one particularly relevant example.[2a]

Such disparate activation parameters between atropinversion in **3a**−**e** and **4·Cl₂** clearly shows that the ligand set trans to the *tropos*-diphosphine exerts a marked influence on the barrier to this process. On this evidence, we suggest that the difference in rates between [(BIPHEP)$RuCl_2$\{(*S*,*S*)-DPEN\}] and [(BIPHEP)-Pt\{(*S*)-BINOL\}] is more likely to be associated with the change from DPEN to BINOL trans to BIPHEP and not unfavorable interactions between the apical chloride ligands and pseudoaxial P−Ph groups, as has been suggested.[4] In considering possible causes for the difference in activation parameters, we note that substitution of BINOL-ate for DPEN results in a slight lengthening of the Pt−P bonds, as evidenced by the average bond lengths of 2.228 and 2.239 Å in **3c** and **4·[CF_3SO_3]₂**, respectively. Although a decrease in the strength of the Pt−P bond could act to reduce the barrier to atropinversion by facilitating the attenuation of strain in the planar cyclic transition state, such a marked increase in rate could also be taken as evidence for a change in mechanism to the off-metal process, as either a direct result of destablization of the ground state and/or a conjugate-base type process in which π-donation from an amide stabilizes the transition state to Pt−P bond dissociation, as shown in Scheme 2. In fact, it should also be noted that π-donation could account for attenuation of strain in the planar transition state by lengthening of the Pt−P bonds. Thus, while the kinetic data do not allow us to distinguish between the two possible mechanisms, the markedly disparate values of $\Delta H^{\ddagger}$ between **4·Cl₂** and **3a**−**e** could indicate that different mechanisms operate.

Chart 3

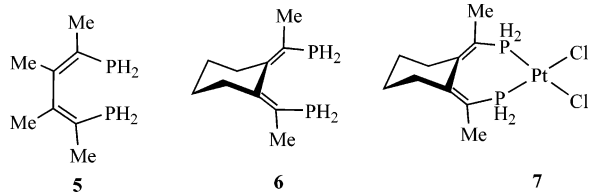

Computational Analysis. In an attempt to understand the influence of coordination to a metal on the barrier to atropinversion, an ab initio study involving model diphosphines and their platinum complexes has been undertaken to estimate the activation barrier to axial torsion in the acyclic and monocyclic NUPHOS diphosphines. Chart 3 illustrates the chemical models that have been analyzed. In all the models studied, chlorides were used in place of the BINOL and hydrogen

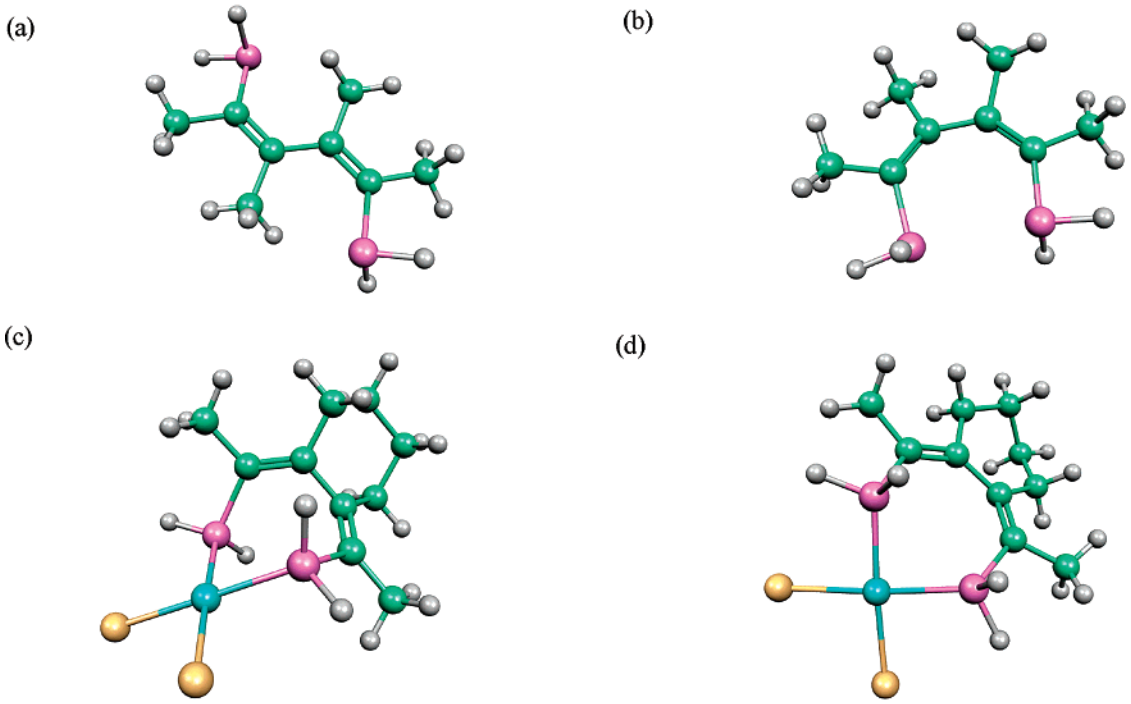

Figure 4. Optimized structures for (a) the planar anti transition state of **5** and (b) the planar syn transition state of **5** using HF and (c) the ground-state structure of **7** and (d) the planar seven-membered metallacycle transition-state structure of **7** using DFT. Color code: Pt, cyan; P, magenta; Cl, yellow; C, green; H, gray.

Table 2. Calculated Energy Differences (kcal mol^{-1}) between the Ground State and Syn Transition State of Model NUPHOS Diphosphines and Platinum Complexes, As Shown in Chart 3

level of theory	**5**	**6**	**7**
HF	32.826	36.745	34.076
DFT		28.696	28.163

atoms were used instead of the phenyl rings attached to the phosphorus atoms, in order to reduce computation time while retaining the essential features of the NUPHOS complexes and free ligands. The energy differences between the ground state and syn transition states of a number of the model NUPHOS diphosphines and their platinum complexes are summarized in Table 2.

In an attempt to explore the off-metal pathway, the transition state corresponding to syn and anti rotation of model **5** have been optimized using HF theory. These calculations revealed that rotation involving an anti transition state (Figure 4a) has a significantly lower barrier (22.154 kcal mol^{-1}) than that of 32.826 kcal mol^{-1} for the syn transition state (Figure 4b) and is in good agreement with calculations performed on 1,1′-binaphthyls.[15] This latter value is similar to that calculated for monocyclic NUPHOS **6** (36.745 kcal mol^{-1}), which can only undergo atropinversion via a syn transition state. Therefore, if atropinversion occurs via Pt−P bond dissociation followed by rotation about C2−C3, it will do so via an anti transition state. Since all the activation barriers determined experimentally for complexes **3a**−**e** are similar, it is reasonable to assume that **3a**−**c** and **3d**,**e** undergo diastereointerconversion via the same mechanism. The fact that neither **3d** or **3e** can rotate about C2−C3 to achieve an anti transition state and that the calculated activation barrier for atropinversion via a syn planar transition state is significantly higher than the experimentally determined value both suggest that atropinversion occurs via the on-metal pathway. Moreover, if we assume that the activation barrier of 32.826 kcal mol^{-1} calculated for atropinversion of **5** is a rough estimate of the barrier to atropinversion via dissociation-induced rotation, this value does not include a contribution from the Pt−P bond dissociation step, which would necessarily raise the barrier quite substantially, especially given the strength of the Pt−P bond. In this regard, a number of previous studies have reported that solvent coordination is important for cleavage of a strong metal−phosphorus bond to occur.[12] However, in the present study a chlorobenzene/toluene mixture has been used as the solvent, which is unlikely to coordinate strongly and therefore cannot assist the bond dissociation process. Therefore, if atropinversion of **3a**−**e** involves a Pt−P bond dissociation step, we could reasonably expect the experimentally determined activation barrier to be even greater than 32.826 kcal mol^{-1}. In considering the on-metal mechanism, the ground and planar metallacycle transition states of model **7** were fully optimized under C_2 symmetry using DFT and the resulting structures are shown in parts c and d Figure 4, respectively. The activation energy of 28.163 kcal mol^{-1} for on-metal atropinversion involving a planar syn transition state is close to the range of experimentally determined values for compounds **3a**−**e**. Thus, each of the factors discussed above combine to indicate that atropinversion in platinum group complexes of NUPHOS-type diphosphines most likely occurs via an on-metal pathway involving a syn transition state.

X-ray Structures of [{1,4-bis(diphenylphosphino)-1,2,3,4-tetramethyl-1,3-butadiene}Pt{(*S*)-BIN-

(15) Kranz, M.; Clark, T.; Schleyer, P. v. R. *J. Am. Chem. Soc.* **1993**, *58*, 3317.

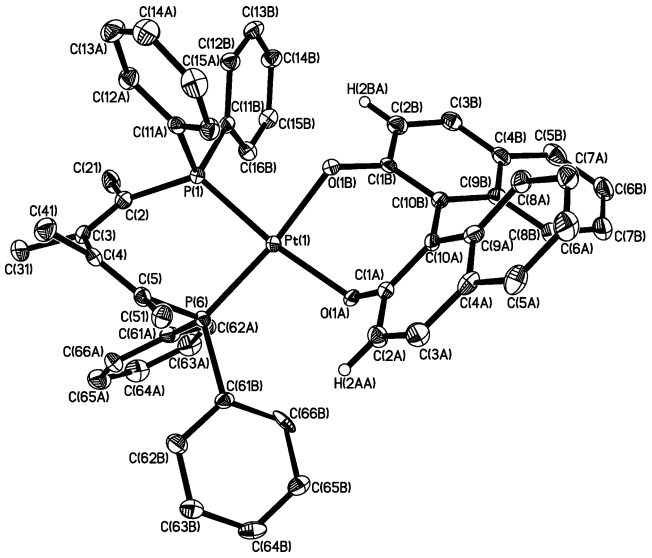

Figure 5. Molecular structure of λ-[(1,2,3,4-Me_4-NUPHOS)-Pt{(*S*)-BINOL}] (λ-(**3a**)), highlighting the mismatched combination of NUPHOS and BINOL stereochemistries. Hydrogen atoms, except for H(2BA) and H(2AA), and dichloromethane molecules of crystallization have been omitted for clarity. Ellipsoids are at the 40% probability level. Selected bond lengths (Å) and angles (deg): Pt(1)−P(1), 2.2350(11); Pt(1)−P(6), 2.2094(11); Pt(1)−O(1A), 2.037(3); Pt(1)−O(1B), 2.060(3); C(2)−C(3), 1.350(6); C(3)−C(4), 1.489(6); C(4)−C(5), 1.330(5); P(1)−Pt(1)−P(6), 88.81(4); O(1A)−Pt(1)−O(1B), 87.13(11); P(6)−Pt(1)−O(1A), 98.53(8); P(6)−Pt(1)−O(1B), 169.27(9); P(1)−Pt(1)−O(1B), 86.13(8); P(1)−Pt(1)−O(1A), 172.03(8).

OL}] (3a) and [{1,2-bis(1-(diphenylphosphino)benzylidene)cyclohexane}Pt{(*S*)-BINOL}] (3e). The disparate thermodynamic stabilities of the enantiopure diastereoisomers of compounds **3a**−**e** prompted us to undertake single-crystal X-ray structure determinations of **3a**,**e** to obtain precise details of the relative stereochemistry of the NUPHOS and BINOL fragments. Perspective views of the molecular structures of **3a**,**e** together with their atomic numbering schemes are shown in Figures 5 and 6, and selected bond lengths and angles for both compounds are listed in the figure captions. The most striking feature of **3a** is the relative stereochemistry of the NUPHOS chelate, which adopts a λ-skew conformation[16] that represents mismatched stereochemistries of NUPHOS and BINOL. The NUPHOS diphosphine coordinates to form a seven-membered chelate ring with a skew-boat conformation, which is highly distorted below the square plane. Gagné has also selectively crystallized the thermodynamically less favored mismatched diastereoisomer λ(*S*)-[(BIPHEP)-Pt{(*S*)BINOL}] and noted that the BIPHEP ligand undergoes a similar distortion to minimize interaction between the pseudoequatorial P−phenyl rings and the 3,3′-C−H bonds of BINOL,[4] which attempt to occupy the same quadrants. This distortion reorientates the phenyl rings away from the classical pseudoaxial and equatorial arrangement commonly found in complexes of BINAP, BIPHEP, and related atropisomeric diphosphines. The two phenyl rings attached to P(1) are evenly disposed above and below the PtP_2 plane, while those attached to P(6) adopt pronounced axial and equatorial positions, such that the latter lies close to the PtP_2 plane. This type of distortion has previously been quantified by the P−Pt−P−C(ipso) dihedral angles, expressed as a rotation above and below the PtP_2 plane. The symmetrically disposed phenyl rings C(11A)−C(16A) and C(11B)−

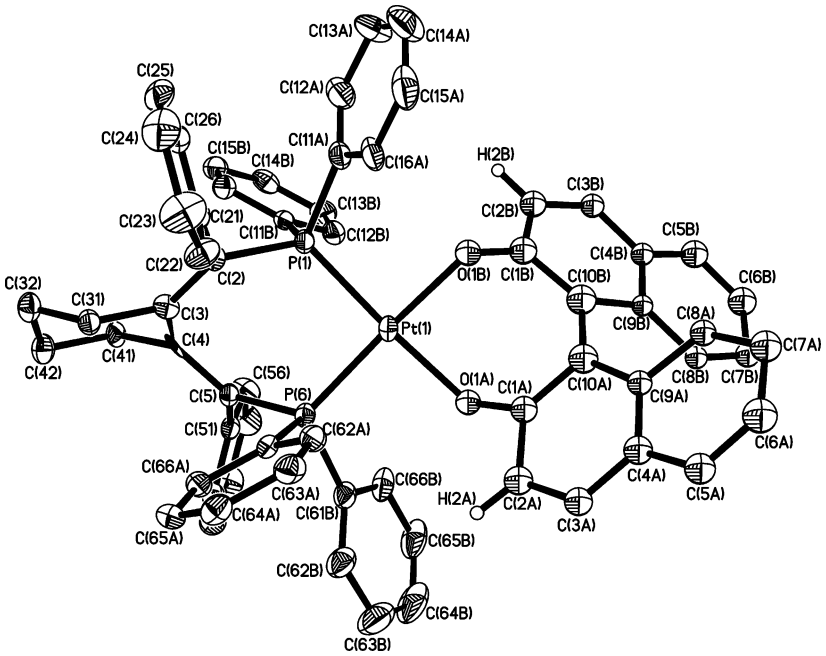

Figure 6. Molecular structure of δ-[(1,4-Ph_2-2,3-*cyclo*-C_6H_8-NUPHOS)Pt{(*S*)-BINOL}] (δ-(**3e**)), showing the relative stereochemistry of the NUPHOS and BINOL fragment as the matched combination. Hydrogen atoms, except for H(2A) and H(2B), and toluene molecules of crystallization have been omitted. Ellipsoids are at the 40% probability level. Selected bond lengths (Å) and angles (deg): Pt(1)−P(1), 2.2235(18); Pt(1)−P(6), 2.2210(19); Pt(1)−O(1A), 2.034(5); Pt(1)−O(1B), 2.037(5); C(2)−C(3), 1.311(9); C(3)−C(4), 1.491(9); C(4)−C(5), 1.389(10); P(1)−Pt(1)−P(6), 92.19(6); O(1A)−Pt(1)−O(1B), 87.79(18); P(6)−Pt(1)−O(1A), 90.59(14); P(6)−Pt(1)−O(1B), 171.82(15); P(1)−Pt(1)−O(1B), 90.56(14); P(1)−Pt(1)−O(1A), 171.50(15); C(2)−C(3)−C(4), 124.8(7); C(3)−C(4)−C(5), 125.3(6); C(2)−C(3)−C(31), 125.6(7); C(31)−C(3)−C(4), 109.2(6); C(41)−C(4)−C(5), 119.4(8); C(3)−C(4)−C(41), 115.1(7).

C(16B) are rotated by 41.2° below and 74.4° above the plane.[4] In contrast, the axial phenyl ring attached to P(6) exposes its edge toward the platinum atom with C(61A)−C(66A) rotated 109.2° above the plane, while its pseudoequatorial counterpart C(61B)−C(66B) is rotated 7.5° below the plane. For comparison the corresponding rotations in [(BIPHEP)Pt{(*S*)-BINOL}] are 73.8 and 44.0° for the symmetric half of the diphosphine and 113 and 6.2° for the more distorted phenyl rings. The distortions present in the solid-state structure of **3a** clearly relate to those in *λ*(*S*)-[(BIPHEP)Pt{(*S*)-BINOL)}] and arise as a result of the mismatched stereochemistries of the BINOL and NUPHOS chelates. The dihedral angles of 61.8° formed between the double bonds and their substituents C(2)C(21)C(3)C(31) and C(4)C(41)C(5)C(51) in **3a** are comparable to those in complexes of related four-carbon-bridged diphosphines.[17] In the case of **3e** the molecular structure confirms the stereochemistry of the NUPHOS and BINOL as matched, with the diphosphine adopting a *δ*-skew conformation. A ^{31}P NMR spectrum of a representative sample of crystals conclusively demonstrated that the X-ray study had been conducted on the thermodynamically favored diastereoisomer. In contrast to the structure of **3a**, in which the NUPHOS and BINOL ligands are highly distorted above the PtP_2 square plane, that of **3e** has close to C_2 symmetry. The platinum atom in **3e** is distorted from an ideal square-planar geometry with a dihedral angle of 11.4° between the PtP_2 and PtO_2 planes. The four rings of the diphenylphosphino groups are arranged in the familiar alternating edge-face manner.[18] The dihedral angle of 56.1° between the least-squares planes containing C(2)C(21)C(3)C(31) and C(4)C(41)C(5)C(51), which describes the atropisomerism of NUPHOS, is similar to that reported for a number of related conformationally restricted diphosphines.[19] Surprisingly, the bonding in the butadiene tether is highly unsymmetrical, with the C(2)−C(3) bond length of 1.311(9) Å significantly shorter that that of 1.389(10) Å associated with C(4)−C(5). The interbond angle of 109.2(6)° at C(3) is significantly smaller than the ideal value of 120° for an sp^2-hybridized carbon and reflects the strong tendency of this carbon atom to adopt an angle close to 109.5° required by a cyclohexane ring. In contrast, the corresponding angle of 115.1(7)° at C(4) is much larger. The natural bite angle of 92.19(6)° is close to the ideal value of 90° and comparable to those reported for [(BIPHEP)$PdCl_2$] (93.03(7)°)[20] and [Pt{(*R*)-BINAP}(*o*-$C_6H_5OMe)_2$] (93.1(1)°).[21]

Conclusions

Diastereointerconversion in the NUPHOS diphosphine complexes [(NUPHOS)Pt{(*S*)-BINOL}] (**3a**−**e**) has been investigated, and Eyring analysis of the resulting rate data gave $\Delta H^{\ddagger}$ values of 22−25 kcal mol^{-1}. Notably, the activation barriers for atropinversion of the acyclic NUPHOS diphosphine complexes **3a**−**c** are similar to those for their monocyclic NUPHOS counterparts **3d**,**e**, which suggest that the same mechanism operates in both cases, either via an on-metal pathway or by Pt−P bond dissociation and syn rotation, since the cyclohexyl ring prevents anti rotation. Combined, kinetic studies and computational analysis indicate that atropinversion of **3a**−**e** most likely occurs via an on-metal pathway involving a cyclic seven-membered transition state. These studies have shown that the conformational stability of the diphosphine stereochemistry in [(NUPHOS)Pt{(*S*)-BINOL}] is similar to that of BIPHEP in [(BIPHEP)Pt{(*S*)-BINOL}]. In a comparative kinetic study the ligand that is trans to the *tropos* diphosphine has been shown to affect the barrier to diastereointerconversion, since substitution of (*S*)-BINOL for (*S*,*S*)-DPEN results in a significant increase in the rate of atropinversion of NUPHOS and a $\Delta H^{\ddagger}$ value of 17 kcal mol^{-1} has been determined for [(NUPHOS)Pt{(*S*,*S*)-DPEN}]Cl_2 (**4·Cl$_2$**), which is much closer to that reported for [(BIPHEP)$RuCl_2${(*S*,*S*)-DPEN}]. On the basis of the similarity between BIPHEP- and NUPHOS-type diphosphines we have initiated a catalyst testing program to explore the applications of these conformationally flexible diphosphine in platinum group asymmetric Lewis acid catalysis.

Experimental Section

General Procedures. All manipulations involving air-sensitive materials were carried out using standard Schlenk line techniques under an atmosphere of nitrogen or argon in oven-dried glassware. Diethyl ether and hexane were distilled from potassium/sodium alloy, tetrahydrofuran from potassium, dichloromethane from calcium hydride, and methanol from magnesium. Unless otherwise stated, commercially purchased materials were used without further purification. The platinum complex [Pt(COD)Cl_2][22] and the NUPHOS[8] diphosphines were prepared as previously described. Deuteriochloroform was predried with calcium hydride, vacuum transferred, and stored over 4 Å molecular sieves. ^{1}H, ^{31}P{^{1}H}, and ^{13}C{^{1}H} NMR spectra were recorded on a JEOL LAMBDA 500 or Bruker AC 200, AMX 300, and DRX 500 machines. Optical rotations were measured on a Perkin-Elmer 241 spectropolarimeter and are reported as follows: $[\alpha]_D$ (*c* in units of g/100 mL, solvent).

Synthesis of Dichloro[1,4-bis(diphenylphosphino)-1,2,3,4-tetramethyl-1,3-butadiene]platinum (2a). A solution of [(cyloocta-1,5-diene)$PtCl_2$] (0.50 g, 1.3 mmol) in dichloromethane (20 mL) was added to a dichloromethane solution of 1,4-bis(diphenylphosphino)-1,2,3,4-tetramethyl-1,3-butadiene (0.635 g, 1.3 mmol), and the mixture was stirred vigorously for 4 h. The reaction mixture was filtered and the solvent removed to leave a pale yellow solid residue. Crystallization by slow diffusion of *n*-hexane into a dichloromethane solution at room temperature gave **2a** as colorless prisms in 88% yield (0.87 g). ^{31}P{^{1}H} NMR (121.5 MHz, $CDCl_3$, *δ*): 6.7 (t, J_{PtP} = 3660 Hz, PPh_2). ^{1}H NMR (300.0 MHz, $CDCl_3$, *δ*): 8.36 (br, 4H,

(16) Brunkan, N. M.; White, P. S.; Gagné, M. R. *Angew. Chem., Int. Ed.* **1998**, *37*, 1579.

(17) (a) Schmid, R.; Firicher, J.; Cereghetti, M.; Schonholzer, P. *Helv. Chim. Acta* **1991**, *74*, 370. (b) Schmid, R.; Cereghetti, M.; Schonholzer, P.; Hansen, H.-J. *Helv. Chim. Acta* **1988**, *71*, 897. (c) Schmid, R.; Broger, E.; Cereghetti, M.; Crameri, Y.; Foricher, J.; Lalonde, M.; Muller, R. K.; Scalone, M.; Schoettel, G.; Zutter, U. *Pure Appl. Chem.* **1996**, *68*, 131. (d) Toriumi, K.; Ito, T.; Takaya, T.; Noyori, R. *Acta Crystallogr.* **1982**, *B38*, 807.

(18) (a) Ozawa, F.; Kubo, A.; Matsumoto, Y.; Hayashi, T.; Nishioka, E.; Yangi, K.; Moriguchi, K. *Organometallics* **1993**, *12*, 4188. (b) Tominaga, H.; Sakai, K.; Tsubomura, T. *J. Chem. Soc., Chem. Commun.* **1995**, 2273.

(19) Ogasawara, M.; Yoshida, K.; Hayashi, T. *Organometallics* **2000**, *19*, 1567.

(20) (a) Alcock, N. W.; Brown, J. M.; Perez-Torrente, J. *Tetrahedron Lett.* **1992**, *33*, 389. (b) Brown, J. M.; Perez-Torrente, J. J.; Alcock, N. W. *Organometallics* **1995**, *14*, 1195.

(21) (a) Gugger, P.; Limmer, S. O.; Watson, A. A.; Willis, A. C.; Wild, S. B. *Inorg. Chem.* **1993**, *32*, 5692. (b) Morton, D. A. V.; Orpen, A. G. *J. Chem. Soc., Dalton Trans.* **1992**, 641.

(22) (a) Drew, D.; Doyle, J. R. *Inorg. Synth.* **1990**, *28*, 246. (b) Chatt, J.; Vallarino, L. M.; Venanzi, L. M. *J. Chem. Soc.* **1957**, 3413.

C_6H_5), 7.58 (m, 8H, C_6H_5), 7.27 (m, 8H, C_6H_5), 1.23 (d, J_{PH} = 11.2 Hz, 6H, CH_3), 1.18 (s, 6H, CH_3). $^{13}C\{^1H\}$ NMR (75.4 MHz, $CDCl_3$, δ): 149−124 (m, C_6H_5 + C=C), 19.5 (t, J_{PC} = 3.3 Hz, CH_3), 17.5 (t, J_{PC} = 5.6 Hz, CH_3). Anal. Calcd for $C_{32}H_{32}Cl_2P_2Pt$: C, 51.62; H, 4.33. Found: C, 51.96; H, 4.44.

Dichloro[1,4-bis(diphenylphosphino)-1,2,3,4-tetraethyl-1,3-butadiene]platinum (2b). Compound **2b** was prepared according to the procedure described above for **2a** and isolated as yellow crystals in 82% yield by slow diffusion of a chloroform solution layered with hexane. $^{31}P\{^1H\}$ NMR (121.5 MHz, $CDCl_3$, δ): 4.6 (t, J_{PtP} = 3814 Hz, PPh_2). ^1H NMR (500.13 MHz, $CDCl_3$, δ): 8.60 (br, 2H, C_6H_5), 7.56−7.09 (m, 18H, C_6H_5), 2.23 (m, 2H, CH_2), 1.75 (br m, 2H, CH_2), 1.45 (br m, 4H, CH_2), 1.03 (t, J = 7.0 Hz, 6H, CH_3), 0.30 (t, J = 7.0 Hz, 6H, CH_3). Anal. Calcd for $C_{36}H_{40}Cl_2P_2Pt$: C, 54.01; H, 5.04. Found: C, 54.36; H, 5.19.

Dichloro[1,4-bis(diphenylphosphino)-1,2,3,4-tetraphenyl-1,3-butadiene]platinum (2c). Compound **2c** was prepared according to the procedure described above for **2a** and isolated as yellow crystals in 79% yield by slow diffusion of a chloroform solution layered with methanol. $^{31}P\{^1H\}$ NMR (121.5 MHz, $CDCl_3$, δ): 1.9 (t, J_{PtP} = 3607 Hz, PPh_2). ^1H NMR (500.13 MHz, $CDCl_3$, 193 K, δ): 9.57 (br m, 2H, C_6H_5), 8.41 (br m, 2H, C_6H_5), 8.0 (br, 6H, C_6H_5), 7.12 (t, J = 7.0 Hz, 2H, C_6H_5), 6.94 (m, 4H, C_6H_5), 6.85 (m, 4H, C_6H_5), 6.80 (t, J = 7.2 Hz, 2H, C_6H_5), 6.77 (t, J = 7.2 Hz, 2H, C_6H_5), 6.65 (t, J = 7.3 Hz, 2H, C_6H_5), 6.56 (t, J = 7.7 Hz, 2H, C_6H_5), 6.60 (t, J = 7.0 Hz, 2H, C_6H_5), 6.18 (d, J = 7.8 Hz, 4H, C_6H_5), 6.06 (d, J = 7.8 Hz, 2H, C_6H_5), 5.94 (d, J = 7.3 Hz, 2H, C_6H_5). Anal. Calcd for $C_{52}H_{40}Cl_2P_2Pt$: C, 62.91; H, 4.06. Found: C, 63.11; H, 4.21.

Dichloro[1,2-bis((diphenylphosphino)ethylmethylene)-cyclohexane]platinum (2d). Compound **2d** was prepared according to the procedure described above for **2a** and isolated as yellow crystals in 71% yield by slow diffusion of a chloroform solution layered with hexane. $^{31}P\{^1H\}$ NMR (121.5 MHz, $CDCl_3$, δ): 5.2 (t, J_{PtP} = 3648 Hz, PPh_2). ^1H NMR (300 MHz, $CDCl_3$, δ): 8.19 (br, 4H, C_6H_5), 7.56−6.98 (m, 16H, C_6H_5), 1.34 (m, 4H, Cy H_2 + CH_2CH_3), 0.92 (br m, 2H, Cy H_2), 0.85 (m, 2H, CH_2CH_3), 0.71 (br m, 4H, Cy H_2), 0.13 (t, J_{PH} = 7.2 Hz, CH_2CH_3). $^{13}C\{^1H\}$ NMR (125.65 MHz, $CDCl_3$, δ): 156−129 (m, C_6H_5), 36.2 (s, Cy CH_2), 29.1 (s, Cy-CH_2), 26.1 (t, J_{PC} = 5.2 Hz, CH_2CH_3), 14.8 (s, CH_2CH_3). Anal. Calcd for $C_{36}H_{38}Cl_2P_2Pt$: C, 54.14; H, 4.80. Found: C, 54.21; H, 4.89.

Dichloro[1,2-bis((diphenylphosphino)phenylmethylene)cyclohexane]platinum (2e). Compound **2e** was prepared according to the procedure described above for **2a** and isolated as yellow crystals in 67% yield by slow diffusion of a chloroform solution layered with hexane. $^{31}P\{^1H\}$ NMR (121.5 MHz, $CDCl_3$, δ): 1.2 (t, J_{PtP} = 3665 Hz, PPh_2). ^1H NMR (500.13 MHz, $CDCl_3$, δ): 8.57 (br, 4H, C_6H_5), 7.76 (br, 6H, C_6H_5), 7.0 (t, J = 7.5 Hz, 2H, C_6H_5), 6.96 (t, J = 7.2 Hz, 2H, C_6H_5), 6.89 (t, J = 7.4 Hz, 2H, C_6H_5), 6.78 (t, J = 7.1 Hz, 2H, C_6H_5), 6.75 (m, 2H, C_6H_5), 6.25 (t, J = 7.4 Hz, 2H, C_6H_5), 6.21 (d, J = 7.3 Hz, 2H, C_6H_5), 5.94 (t, J = 7.3 Hz, 2H, C_6H_5), 1.86 (d, J = 13.4 Hz, 2H, Cy CH_2), 1.56 (br, 2H, Cy CH_2), 1.47 (br, 2H, Cy CH_2), 1.19 (br t, J = 9.0 Hz, 2H, Cy CH_2). Anal. Calcd for $C_{44}H_{38}Cl_2P_2Pt\cdot 4CHCl_3$: C, 42.01; H, 3.09. Found: C, 41.23; H, 2.33.

Synthesis of [{1,4-bis(diphenylphosphino)-1,2,3,4-tetramethyl-1,3-butadiene}platinum{(*S*)-BINOL}] (3a). A solution of (*S*)-BINOL (0.383 g, 1.34 mmol) in tetrahydrofuran (30 mL) was slowly added to a rapidly stirred solution of freshly sublimed sodium *tert*-butoxide (0.259, g 2.70 mmol) in THF (30 mL). After the mixture was stirred for ca. 15 min, the resulting solution was transferred via cannula to a suspension of **2a** (1.0 g, 1.34 mmol) in toluene (30 mL), which resulted in the immediate appearance of an orange coloration. The reaction mixture was stirred for 90 min, during which time the solid dissolved to give an intense orange solution. The reaction mixture was filtered and the solvent removed to give a deep orange solid, which was extracted into chloroform and filtered to remove sodium chloride. The solvent was removed and the resulting orange solid triturated with hexane to afford the desired product as a 1:1 mixture of diastereoisomers in 79% yield (1.01 g). Crystallization by slow diffusion of a dichloromethane solution layered with *n*-hexane gave X-ray-quality crystals of the thermodynamically less favored diastereoisomer only. $^{31}P\{^1H\}$ NMR (121.5 MHz, $CDCl_3$, δ): 3.0 (t, J_{PtP} = 3668 Hz, PPh_2). ^1H NMR (500.13 MHz, $CDCl_3$, δ): 7.99 (t, J = 3.2 Hz, 6H aromatic), 7.65 (d, J = 7.95 Hz, 2H, aromatic), 7.46−7.42 (m, 8H, aromatic), 7.27−7.22 (m, 8H, aromatic), 7.07 (d, J = 7.9 Hz, 2H, aromatic), 7.03 (d, J = 8.1 Hz, 2H, aromatic), 6.98 (d, J = 8.8 Hz, 2H, aromatic), 6.31 (d, J = 8.8 Hz, 2H, aromatic), 1.41 (d, J = 5.6 Hz, 6H, CH_3), 1.16 (s, 6H, CH_3). Anal. Calcd for $C_{52}H_{44}O_2P_2Pt$: C, 65.20; H, 4.63. Found: C, 65.09; H, 4.32. $[\alpha]_D$ = −0.92° (*c* 1.0, $CHCl_3$).

[{1,4-bis(diphenylphosphino)-1,2,3,4-tetraethyl-1,3-butadiene}platinum{(*S*)-BINOL}] (3b). Compound **3b** was prepared according to the procedure described above for **3a** and isolated as an orange solid in 88% yield. $^{31}P\{^1H\}$ NMR (121.5 MHz, $CDCl_3$, δ): 0.4 (t, J_{PtP} = 3700 Hz, PPh_2), −2.3 (t, J_{PtP} = 3630 Hz, PPh_2). ^1H NMR (500.13 MHz, $CDCl_3$, δ): 8.22 (br, aromatic), 8.02 (br t, J = 13.0 Hz, aromatic), 7.71 (t, J = 12.0 Hz, aromatic), 7.61−6.9 (m, aromatic), 6.69 (d, J = 14.5 Hz, aromatic), 6.15 (d, J = 14.6 Hz, aromatic), 2.01 (m 2H, CH_aH_b), 1.90 (m, 4H, CH_cH_d + CH_eH_f), 1.81 (m, 2H, CH_aH_b), 1.48 (m, 4H, CH_cH_d + CH_gH_i), 1.32 (m, 2H, CH_eH_f), 1.26 (m, 2H, CH_gH_i), 1.01 (t, J = 7.5 Hz, 3H, CH_2CH_3), 0.87 (t, J = 7.5 Hz, 3H, CH_2CH_3), 0.58 (t, J = 7.4 Hz, 3H, CH_2CH_3), 0.23 (t, J = 7.4 Hz, 3H, CH_2CH_3). Anal. Calcd for $C_{56}H_{52}O_2P_2Pt$: C, 66.33; H, 5.17. Found: C, 66.67; H, 5.44. $[\alpha]_D$ = −8.9° (*c* 1.0, $CHCl_3$).

[{1,4-bis(diphenylphosphino)-1,2,3,4-tetraphenyl-1,3-butadiene}platinum{(*S*)-BINOL}] (3c). Compound **3c** was prepared according to the procedure described above for **3a** and isolated as an intense yellow solid in 63% yield. Crystallization by slow diffusion of *n*-hexane into a dichloromethane solution at room temperature gave X-ray-quality crystals of the thermodynamically preferred diastereoisomer. $^{31}P\{^1H\}$ NMR (121.5 MHz, $CDCl_3$, δ): −1.0 (t, J_{PtP} = 3619 Hz, PPh_2). ^1H NMR (500.13 MHz, $CDCl_3$, δ): 8.98 (br, 4H, aromatic), 7.9 (br, 6H, aromatic), 7.64 (d, J = 8.2 Hz, 2H, aromatic), 7.46 (d, J = 8.8 Hz, 2H, aromatic), 7.02 (t, J = 6.7 Hz, 2H, aromatic), 6.94−6.91 (m, 6H, aromatic), 6.87 (t, J = 6.9 Hz, aromatic), 6.76 (m, 6H, aromatic), 6.70 (br, 2H, aromatic), 6.63 (t, J = 7.3 Hz, 4H, aromatic), 6.56 (m, 6H, aromatic), 6.4 (br, 2H, aromatic), 6.14 (br, 4H, aromatic), 6.02 (d, J = 7.2 Hz, 4H, aromatic). Anal. Calcd for $C_{72}H_{52}O_2P_2Pt$: C, 71.69; H, 4.35. Found: C, 71.87; H, 4.48. $[\alpha]_D$ = −11.1° (*c* 1.0, $CHCl_3$).

[{1,2-bis((diphenylphosphino)ethylmethylene)cyclohexane}platinum{(*S*)-BINOL}] (3d). Compound **3d** was prepared according to the procedure described above for **3a** and isolated as an orange solid in 69% yield. Crystallization from a toluene solution at room temperature gave X-ray-quality crystals of the thermodynamically preferred diastereoisomer. $^{31}P\{^1H\}$ NMR (121.5 MHz, $CDCl_3$, δ): −0.4 (t, J_{PtP} = 3700 Hz, PPh_2), −1.7 (t, J_{PtP} = 3648 Hz, PPh_2). ^1H NMR single diastereoisomer (500.13 MHz, $CDCl_3$, δ): 8.17 (br, 4H, aromatic), 7.9−6.89 (m, 26H, aromatic), 6.53 (d, J = 8.7 Hz, 2H, aromatic), 2.13−0.81 (m, 12H, Cy H_2 + CH_2CH_3), 0.31 (t, J = 7.4 Hz, 6H, CH_2CH_3). Anal. Calcd for $C_{56}H_{50}O_2P_2Pt\cdot 2C_7H_8$: C, 70.28; H, 5.56. Found: C, 70.67; H, 5.73. $[\alpha]_D$ = −4.6° (*c* 1.0, $CHCl_3$).

[{1,2-bis((diphenylphosphino)phenylmethylene)-cyclohexane}platinum{(*S*)-BINOL}] (3e). Compound **3e** was prepared according to the procedure described above for **3a** and isolated as an intense yellow solid in 67% yield. Crystallization from a toluene−dichloromethane solution at room temperature gave X-ray-quality crystals of the thermodynamically preferred diastereoisomer. $^{31}P\{^1H\}$ NMR (121.5 MHz, $CDCl_3$, δ): −0.8 (t, J_{PtP} = 3667 Hz, PPh_2). ^1H NMR (500.13 MHz, $CDCl_3$, δ): 8.59 (br m, 4H, aromatic), 7.70 (m, 4H, aromatic), 7.51 (d, J = 8.8 Hz, 2H, aromatic), 7.40 (d, J =

8.8 Hz, 2H, aromatic), 7.19−7.10 (m, 4H, aromatic), 6.92 (t, J = 7.5 Hz, 2H, aromatic), 6.86−6.76 (m, 12H, aromatic), 6.67 (t, J = 5.3 Hz, 4H, aromatic), 6.60 (t, J = 6.9 Hz, 2H, aromatic), 6.52 (t, J = 8.7 Hz, 2H, aromatic), 6.07 (d, J = 7.55 Hz, 2H, aromatic), 6.03 (d, J = 8.0 Hz, 2H, aromatic), 1.84 (br d, 2H, Cy-H_2), 1.46 (br m, 4H, Cy H_2), 1.18 (br, 2H, Cy H_2). Anal. Calcd for $C_{64}H_{50}O_2P_2Pt{\cdot}2C_7H_8$: C, 72.49; H, 5.15. Found: C, 72.83; H, 5.54. $[\alpha]_D = -4.7°$ (*c* 1.0, $CHCl_3$).

Synthesis of [{1,4-bis(diphenylphosphino)-1,2,3,4-tetraphenyl-1,3-butadiene}platinum{(*S*,*S*)-DPEN}]Cl_2 (4·Cl_2). A dichloromethane solution of (*S*,*S*)-1,2-diphenylethylenediamine (0.053 g, 0.25 mmol in 5 mL) was added to a stirred solution of enantiopure δ-[(Ph_4-NUPHOS)$PtCl_2$] (0.25, 0.25 mmol) in dichloromethane. After 30 min the reaction mixture was filtered, the solvent removed, and the residue crystallized from a dichloromethane solution layered with hexane to give **4·Cl_2** in 77% yield (0.233 g). $^{31}P\{^1H\}$ NMR (121.5 MHz, $CDCl_3$, δ): −6.5 (t, J_{PtP} = 3315 Hz, PPh_2). ^1H NMR (500.13 MHz, $CDCl_3$, δ): 8.11 (br, 4H, aromatic), 8.04 (t, J = 6.4 Hz, 2H, aromatic), 7.44 (d, J = 6.8 Hz, 6H, aromatic), 7.16 (m, 6H, aromatic), 7.06 (m, 10H, aromatic), 6.82 (t, J = 7.4 Hz, 2H, aromatic), 6.71 (t, J = 6.4 Hz, 2H, aromatic), 6.33 (m, 6H, aromatic), 6.59 (t, J = 7.4 Hz, 2H, aromatic), 6.21 (d, J = 7.8 Hz, 2H, aromatic), 6.05 (d, J = 7.2 Hz, 4H, aromatic), 5.72 (br m, 2H, NH_2CH), 5,67 (br, 2H, NH_aH_b), 3.20 (br d, 2H, NH_aH_b). Anal. Calcd for $C_{66}H_{56}Cl_2N_2P_2Pt$: C, 72.49; H, 5.15. Found: C, 72.83; H, 5.54. Crystals of **4·[CF_3SO_3]$_2$** suitable for X-ray analysis were obtained by reaction of **4·Cl_2** with 2 equiv of silver trifluoromethanesulfonate in dichloromethane followed by crystallization from a chloroform solution layered with *n*-hexane at room temperature.

Kinetic Study of the Thermal Interconversion of λ-(*S*)-3a−e to δ(*S*)-3a−e. In a typical procedure a 1:1 diastereoisomeric mixture of **3a** (10.4 mg, 10.6 μmol) was dissolved in a mixture of chlorobenzene (0.35 mL) and d_8-toluene (0.15 mL) and placed in an NMR tube. A time zero spectrum was recorded, the sample was heated at the specified temperature for a known amount of time and quenched in an ice bath, and a $^{31}P\{^1H\}$ spectrum was recorded. In this manner the progress of the thermal diastereointerconversion of λ(*S*)-**3a**−**e** to δ(*S*)-**3a**−**e** was monitored.

Chemical Models and Computational Studies. Initially, Hartree−Fock (HF) level calculations were used to optimize the structures. Further optimization was performed first using Møller−Plesset second-order perturbation theory (MP2) and using density functional theory (DFT). All the HF level calculations were performed on the PC version of GAMESS[23,25] (version 6.1; build 2032), while the DFT level (B3LYP functional)[24] calculations were performed on the UNIX based version[25] running on a Cygwin[26] client (GAMESS version released June 20, 2002, R1). Initially all calculations (except DFT level) were performed using the effective core potential basis set by Stevens et al.[27] (valence double-ζ), which is part of the GAMESS package. For the determination of better thermodynamic properties on the chemically more relevant models, calculations were repeated using the LanL2DZ effective core potential basis set[28] (which was also used for DFT level calculations) available from the EMSL database.[29] Effective core potentials were used throughout to facilitate computation of systems that included the metal and to make comparison with free ligand calculations possible. All optimizations were checked, using vibrational analysis, to ensure that the minima on the potential energy surface were true local minima (by ensuring the second-derivative Hessian matrix was positive definite) and that all transition state structures had only one imaginary vibrational frequency. Furthermore, intrinsic reaction coordinate following was performed to link the transition-state structures to the structural minima.

Crystal Structure Determinations of 3a and 3e. Data were collected on a Bruker-AXS SMART diffractometer using the SAINT-NT software[30] with graphite-monochromated Mo Kα radiation using ψ/ω scans. A crystal was mounted onto the diffractometer at low temperature under dinitrogen at ca. 120 K. Crystal stabilities were monitored via re-collection of the first set of frames. There were no significant variations (<±1%). Lorentz and polarization corrections were applied. The structures were solved using direct methods and refined with the SHELXTL program package,[31] and the non-hydrogen atoms were refined with anisotropic thermal parameters. Hydrogen atoms were added at idealized positions, and a riding model was used for subsequent refinement. Although the structure of **3e** can be solved in both $P3_1$ and $P3_12_1$, the space group $P3_1$ was chosen over $P3_12_1$ because the disorder in the model is reduced to being only associated with the BINOL-ate ligand and this resulted in a better fit for the data (i.e. R1 = 0.0454 for $P3_1$ and R1 = 0.0856 for $P3_12_1$). The function minimized was $\sum[w(|F_o|^2 - |F_c|^2)]$, with reflection weights $w^{-1} = [\sigma^2|F_o|^2 + (g_1P)^2 + (g_2P)]$, where $P = [\max |F_o|^2 + 2|F_c|^2]/3$. Additional material available from the Cambridge Crystallographic Data Center comprises relevant tables of atomic coordinates, bond lengths and angles, and thermal parameters.

Acknowledgment. We gratefully acknowledge the EPSRC (R.K.R.), CenTACat, and the McClay Trust (C.R.N.) for funding and Johnson Matthey for loans of palladium salts. J.A.v.d.B. thanks SASOL Research and Development for sponsorship (Grant R8112QLL).

Supporting Information Available: Text giving reversible first-order analyses for the thermal isomerization of λ(*S*)-**3b**−**d** to δ(*S*)-**3b**−**d** and δ(*S*,*S*)-**4·Cl_2** to λ(*S*,*S*)-**4·Cl_2**, rate constant data, k (s^{-1}), obtained for the atropisomerization of compounds **3a**−**d** and **4**, and tables of crystal data, structure solution and refinement, atomic coordinates, bond distances, bond angles, and anisotropic thermal parameters and perspective views for compounds **3a**,**c**,**e** and **4·[CF_3SO_3]$_2$**. This material is available free of charge via the Internet at http://pubs.acs.org. Observed and calculated structure factor tables are available from the authors upon request.

OM034289F

(23) Granovsky, A. A. Available from http://classic.chem.msu.su/gran/gamess/index.html.

(24) (a) Becke, A. D. *J. Chem. Phys.* **1993**, *98*, 5648. (b) Stephens, P. J.; Devlin, F. J.; Chablowski, C. F.; Frisch, M. J. *J. Phys. Chem.* **1994**, *98*, 11623. (c) Hertwig, R. H.; Koch, W. *Chem. Phys. Lett.* **1997**, *268*, 345.

(25) Schmidt, M. W.; Baldridge, K. K.; Boatz, J. A.; Elbert, S. T.; Gordon, M. S.; Jensen, J. J.; Koseki, S.; Matsunaga, N.; Nguyen, K. A.; Su, S.; Windus, T. L.; Dupuis, M.; Montgomery, J. A. *J. Comput. Chem.* **1993**, *14*, 1346.

(26) Available from http://www.cygwin.com.

(27) (a) Stevens, W. J.; Basch, H.; Krauss, M. *J. Chem. Phys.* **1984**, *81*, 6026. (b) Stevens, W. J.; Krauss, M.; Basch, H.; Jasien, P. G. *Can. J. Chem.* **1992**, *70*, 612. (c) Cundari, T. R.; Stevens, W. J. *J. Chem. Phys.* **1993**, *98*, 5555.

(28) (a) Dunning, T. H., Jr.; Hay, P. J. In *Methods of Electronic Structure Theory*; Schaefer, H. F., Ed.; Plenum Press: New York, 1997; Vol. 2. (b) Hay, P. J.; Wadt, R. W. *J. Chem. Phys.* **1985**, *82*, 270. (c) Hay, P. J.; Wadt, R. W. *J. Chem. Phys.* **1985**, *82*, 284. (d) Hay, P. J.; Wadt, R. W. *J. Chem. Phys.* **1985**, *82*, 299.

(29) Available from http://www.emsl.pnl.gov:2080/forms/basisform.html.

(30) SAINT-NT, Program for Data Collection and Data Reduction; Bruker-AXS, Madison, WI, 1998.

(31) Sheldrick, G. M. SHELXTL Version 5.0, A System for Structure Solution and Refinement; Bruker-AXS, Madison, WI, 1998.